

## THE TURBULENT WAKE OF A SUBMARINE MODEL IN PITCH AND YAW

A. Ashok and A.J. Smits

Department of Mechanical and Aerospace Engineering  
Princeton University  
Princeton, NJ  
aashok@princeton.edu

### Introduction

We aim to improve our understanding of the high Reynolds number wakes formed by maneuvering submarines. When the submarine is pitched or yawed, a complex, three-dimensional separation occurs over the body which results in a non-axisymmetric wake. Studies on wakes have typically been confined to planar or axisymmetric wakes generated by disks, spheres, and other bodies-of-revolution (see, for example, Johannsson and George (2006) and Jimenez et al. (2010)). In contrast, the downstream development of the non-axisymmetric wake has been much less well studied. Lloyd and Campbell (1986), in a study of submarine wakes noted that the azimuthal adverse pressure gradient on a pitched, body-of-revolution causes boundary layer separation, and the separated shear layers then roll up in to streamwise vortices, which increase in strength as more fluid is entrained into the vortex cores until they are shed into the wake with a fixed circulation (see Figure 1). They found that at high angles of incidence asymmetric vortex patterns may be visible but that these angles of incidence are not generally encountered by submarines. As we shall see, such asymmetric wake patterns appear to be characteristic of pitched or yawed bodies of revolution at sufficiently high Reynolds number even at lower angles which may well be encountered by maneuvering submarines.

In another important study, Chesnakas and Simpson (1997) investigated the three-dimensional flow

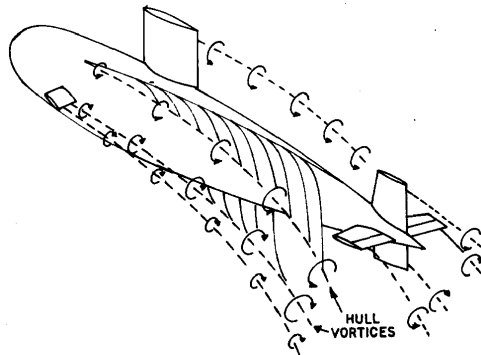


Figure 1. Typical pattern of vortices on a maneuvering submarine Lloyd and Campbell (1986).

separation occurring over a 6:1 prolate spheroid at various pitch angles. Using a three-component LDV system embedded within the body, they measured all three components of the velocity in the three-dimensional boundary layer. They identified the vortex separation points, and used pressure measurements to explain the presence of the secondary vortex first observed by Lloyd and Campbell (1986). More recently, Gross et al. (2011) and Karlsson and Fureby (2009) have performed detailed computations on the DARPA SUBOFF geometry and the prolate spheroid, respectively (the SUBOFF geometry is an idealized submarine shape, see Groves et al. 1989). Gross et al. present vorticity contours and skin-friction lines which are perfectly symmetric since only half the flow was computed and reflected about the centerline. The skin friction lines display the classic primary and secondary separation lines which are visible for all three Reynolds numbers computed. For the higher Reynolds numbers no separation bubble exists, but primary and secondary vortices are present at all Reynolds numbers, although the point at which they form moves downstream with increasing Reynolds number. Karlsson and Fureby (2009) in their study of a prolate spheroid suggest that incorporating a trip wire was as important as accurately resolving the boundary layer growing over the body because any simulations without a trip wire failed to capture the secondary vortex.

Here we present measurements on the wakes generated by a DARPA SUBOFF model over a range of angles of pitch and yaw. The body is held in the wind tunnel by a support formed by extending the sail, as shown in Figure 2. From previous experiments on the same model at zero pitch angle by Jimenez et al. (2010), it was found that the support affects the mean velocity and turbulence profiles in a fairly limited azimuthal region downstream of the support. For the present case, the presence of the support leads to an important distinction between pitch, where the body moves in the plane of the support, and yaw, where the body moves in a plane at right angles to the support.

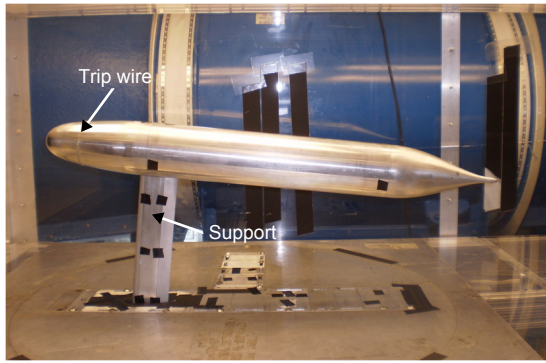


Figure 2. 1:120 DARPA SUBOFF model shown mounted in the wind tunnel in positive pitch. Flow is from left to right.

### Experiments

A 1:120 SUBOFF model without appendages was mounted in a low speed wind tunnel with a test section measuring 0.61 m by 0.91 m and 2.44 m long. The length of the model was 0.87 m with a maximum diameter of 0.102 m. The support was located at the intersection of the fore-body and mid-body sections where the sail would normally be located and had the same cross-section as the sail as specified in the SUBOFF geometry. The boundary layer on the model was tripped 75 mm downstream of the model's nose with a 0.8 mm diameter trip wire. Trip wires of 1.6 mm and 3.2 mm in diameter were also tested to understand the sensitivity of the wake to the size of the trip wire.

Measurements were taken in the near wake, 10 diameters downstream of the stern, at a Reynolds number based on the length of  $2.4 \times 10^6$  (40 m/s). Mean velocity and stream-wise turbulence measurements were performed using Pitot probes and hot wires, respectively. Single component, 0.5 mm Wollaston wires were used with a typical frequency response of 65 kHz at 40 m/s. The probes were mounted on a traverse capable of moving the probes in a plane normal to the flow, as shown in Figure 3. Rotary encoders mounted on the lead screws ensured that an accuracy of  $\pm 0.1$  mm was achieved in both  $y$ - and  $z$ -directions. A total of 900 measurement points were taken in a square grid with spacing of 5 mm, resulting in a 30 by 30 matrix of points. The hot wire and Pitot channels were sampled at 40 kHz for 15 seconds.

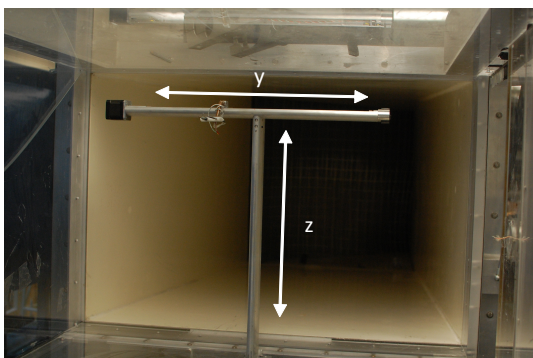


Figure 3. View of traverse system, looking downstream. The  $y$ - $z$  measurement plane is normal to the streamwise flow.

### Results

We start with the axisymmetric (reference) case first. Figures 4, 5 and 6 show the mean streamwise and in-plane flow fields. The flow is approximately axisymmetric as expected. In the lower half of the measurement plane, the presence of the support is apparent. The bimodal distribution in the streamwise turbulence intensity is similar to that found by Jimenez et al. (2010). We note from the vector map that there is a non-zero circulation in the flow. This is perhaps unexpected in what should be an axisymmetric flow. In this convectively unstable flow, a small disturbance (for example on the nose of the submarine) can result in the flow developing an asymmetric mean component that persists far downstream. Though it has been noted that such an asymmetry is accompanied by a side force the patterns that emerge from such an asymmetry have not been studied in detail. For more details see Bridges' extensive review on this issue, see Bridges (2006). Incidentally, the non-zero circulation explains why we see the wake of the support shifted off-center to the left. The magnitude of the in-plane velocity is, however, less than 3 percent of the streamwise velocity, so the circulation is relatively weak.

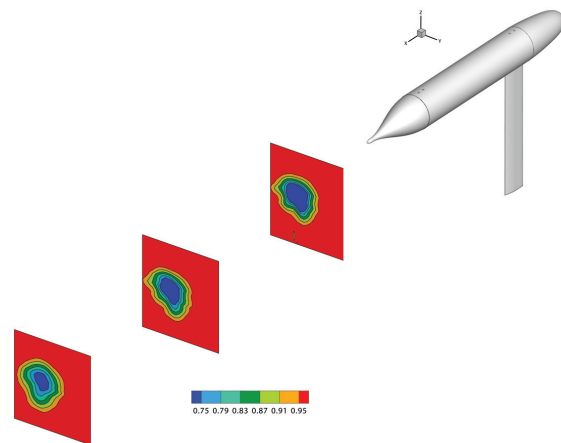


Figure 4. Contours of  $\bar{U}/U_\infty$  for the axisymmetric case.

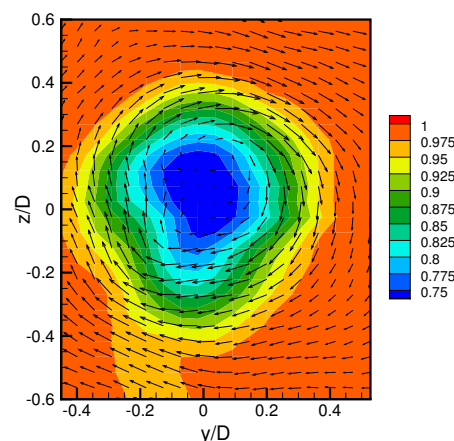


Figure 5. In-plane velocity vectors superimposed on contours of  $\bar{U}/U_\infty$ . Axisymmetric case,  $x/D = 8$ .

A:

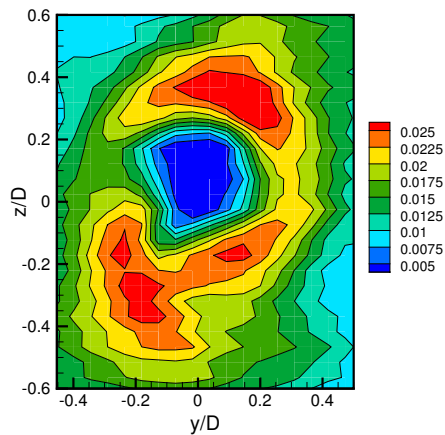


Figure 6. Contours of  $\sqrt{v'^2 + w'^2}/U_\infty$ . Axisymmetric case,  $x/D = 8$ .

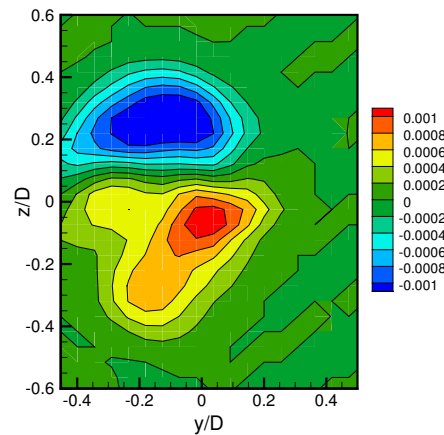


Figure 8. Shear stress  $\overline{u'v'}/U_\infty^2$ . Axisymmetric case,  $x/D = 8$ .

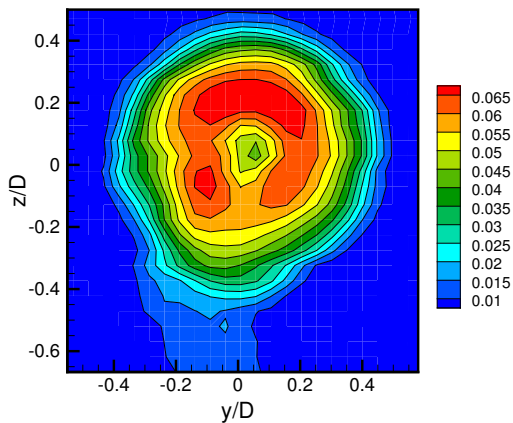


Figure 7. Streamwise velocity fluctuation  $\overline{u'}/U_\infty$ . Axisymmetric case,  $x/D = 8$ .

In Figure 7, the bimodal distribution of the streamwise turbulence intensities is clearly visible and is a consequence of the merging of two shear layers from the top and bottom surfaces of the submarine. The fact that they are not quite symmetric is, as mentioned before, due to the support. The shear stress distribution clearly shows the destructive interference caused by the support which lowers the observed turbulence intensities as seen by Jimenez, Reynolds and Smits (2010). We note that the flow is quite anisotropic, with up to half the turbulent kinetic energy coming from the in-plane components rather than the streamwise component of the velocity. The slight asymmetry in the shear stress magnitudes seen in  $\overline{u'v'}$  is potentially due to the net circulation seen in Figure 5 which would tend to decrease the negative shear stress and increase the positive shear as seen in Figure 8.

For the Pitch = +8° (Figures 9 through 11) and Yaw = ±8° (Figures 12 through 17) cases we present plots similar to the axisymmetric case. The magnitudes of the in-plane velocity as a fraction of the streamwise velocity are also shown. For the pitch case, we can clearly see the presence of a jet between the two vortices that causes fluid to be moved across the wake

between the two vortices. The asymmetry in the vortices is confirmed when computing the circulation.

For the yaw cases we know from flow visualization at lower Reynolds numbers that the separation locations will be on the top and bottom of the submarine as opposed to the pitch cases where the separations occur on the left and right (viewed along the longitudinal axis of the body). We expect to see one steady vortex from the top of the model and one unsteady vortex from the bottom where the support chops up the vortex and causes vortex shedding. We can see that the in-plane measurements are only sensitive to the steady vortex that was likely unaffected by the support. Clearly in an instantaneous realization we expect to see two vortices as in the pitch case with a much weaker unsteady vortex. The steady vortex in yaw is quite strong, it causes sufficient rotation in the flow such that the wake of the support is dragged along as seen in Figures 13 and 16.

It was found that the mean flow patterns are sensitive to the size of the trip wire. This was discovered when attempting to reconcile differences seen in the mean flow patterns between Yaw = 8° and Yaw = -8° using the original 0.8 mm trip wire: see Figures 19 and 20. The data were taken twice to check repeatability. Two other trip wires with  $d = 1.6$  mm and  $d = 3.2$  were also tested. While the Yaw = -8° case was recovered almost independent of the trip diameter, the Yaw = 8° was more like the mirror image of the Yaw = -8° case, with the larger trip wires as shown in Figure 20. Hence, we see that the details of the tripping mechanism can have a significant effect on wake development at this Reynolds number, and that it is necessary to have a large enough trip diameter to ensure left-right symmetry, especially in yaw.

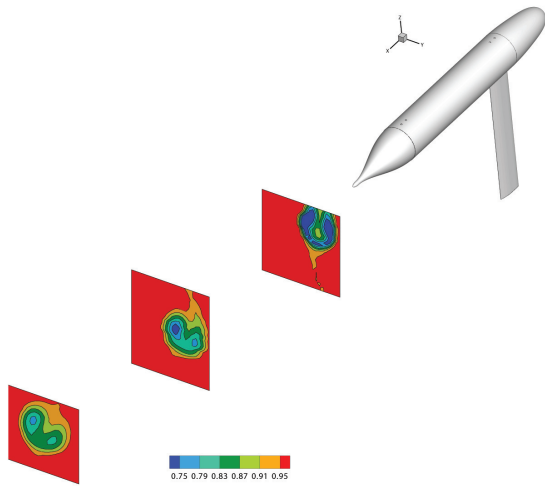


Figure 9. Contours of  $\bar{U}/U_\infty$  for Pitch = +8°.

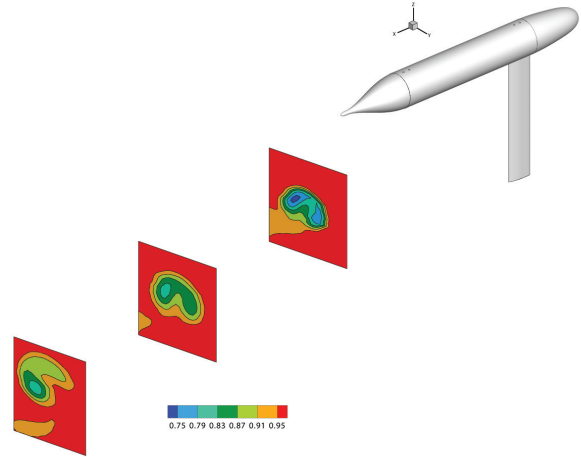


Figure 12. Contours of  $\bar{U}/U_\infty$  for Yaw = +8°.

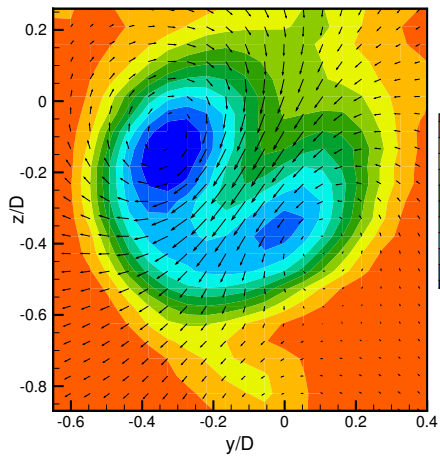


Figure 10. In-plane velocity vectors superimposed on contours of  $\bar{U}/U_\infty$ . Pitch = +8°,  $x/D = 8$ .

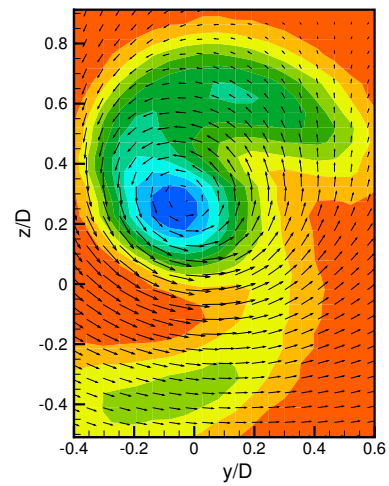


Figure 13. In-plane velocity vectors superimposed on contours of  $\bar{U}/U_\infty$ . Yaw = +8°,  $x/D = 8$ .

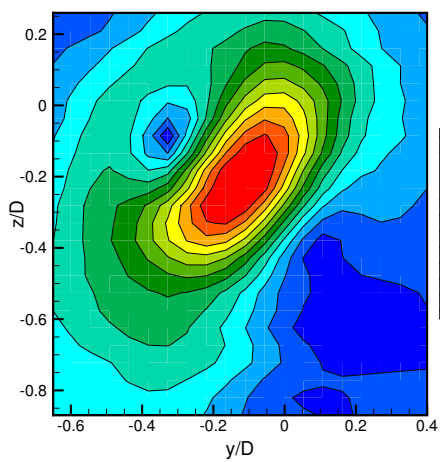


Figure 11. Contours of  $\sqrt{\bar{v}^2 + \bar{w}^2}/U_\infty$ . Pitch = +8°,  $x/D = 8$ .

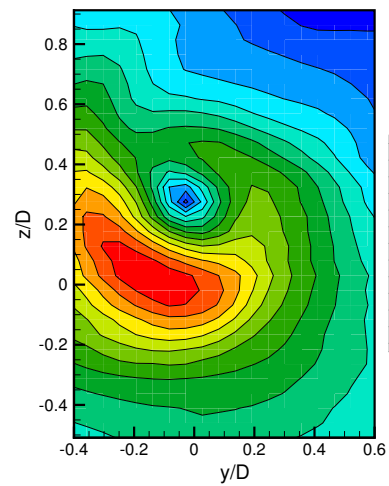


Figure 14. Contours of  $\sqrt{\bar{v}^2 + \bar{w}^2}/U_\infty$ . Yaw = +8°,  $x/D = 8$ .

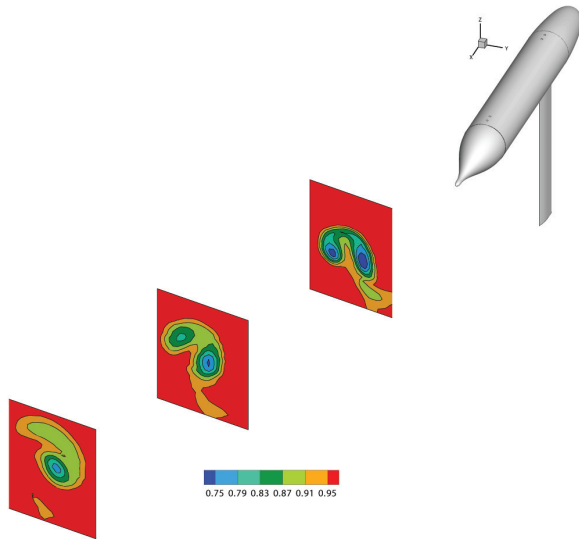


Figure 15. Contours of  $\bar{U}/U_\infty$  for Yaw =  $-8^\circ$ .

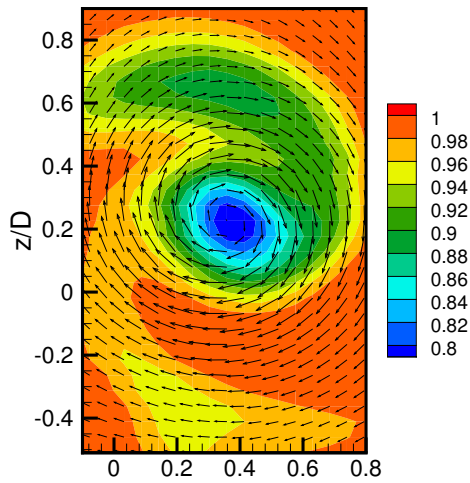


Figure 16. In-plane velocity vectors superimposed on contours of  $\bar{U}/U_\infty$ . Yaw =  $-8^\circ$ ,  $x/D = 8$ .

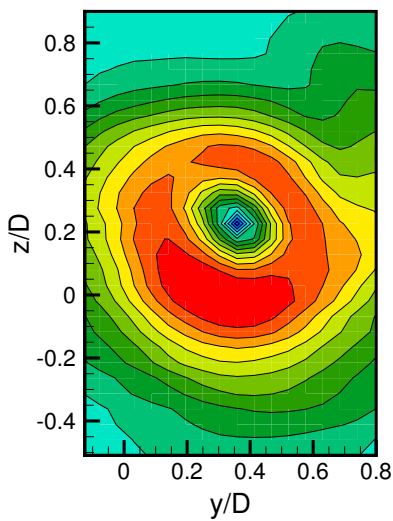


Figure 17. Contours of  $\sqrt{v^2 + w^2}/U_\infty$ . Yaw =  $-8^\circ$ ,  $x/D = 8$ .

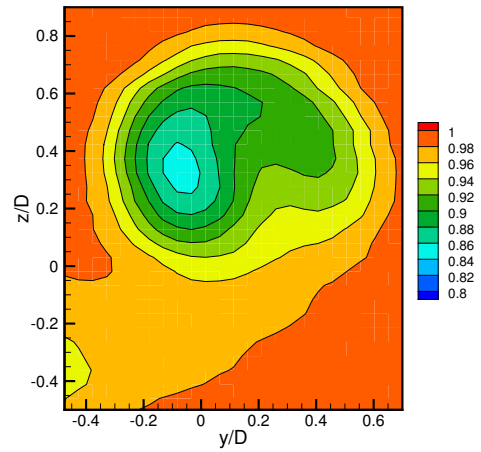


Figure 18.  $\bar{U}/U_\infty$  contours for Yaw =  $+8^\circ$  with 0.8 mm wire.

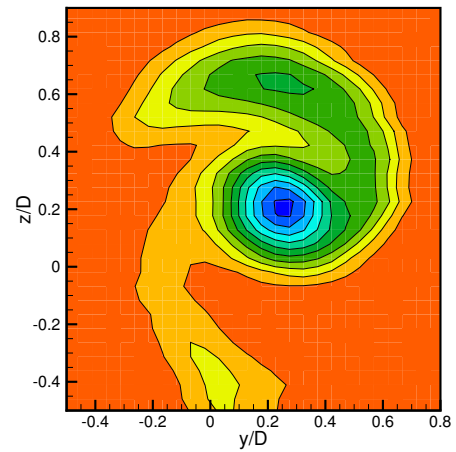


Figure 19.  $\bar{U}/U_\infty$  contours for Yaw =  $-8^\circ$  with 0.8 mm trip wire. For this yaw angle using the 1.6 mm trip wire resulted in virtually the identical pattern.

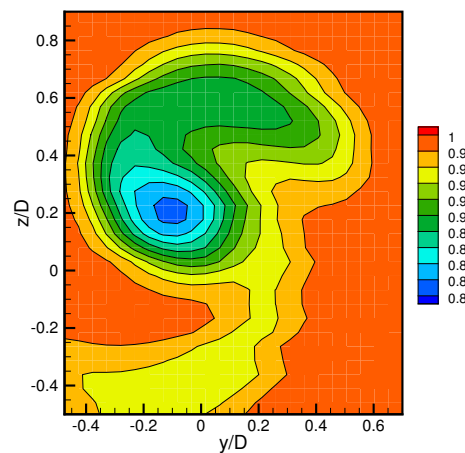


Figure 20.  $\bar{U}/U_\infty$  contours for Yaw =  $+8^\circ$  1.6 mm trip wire.

## Current Work

We are now conducting experiments in the High Reynolds Number Test Facility (HRTF), as shown in Figure 21. This is a pressurized wind tunnel with a circular cross-section capable of generating Reynolds numbers based on the length ( $L = 0.44$  m) of up to  $Re_L = 33.5 \times 10^6$ . More details on the flow facility are given by Jimenez (2007), and Jimenez *et al.* (2010). By comparison, a similar model in a conventional low speed tunnel with a typical maximum speed of about 40 m/s would only be able to achieve an  $Re_L = 1.75 \times 10^6$ , 20 times smaller. Though it has been postulated, see Delery (2001), that the “flow physics do not critically depend on this parameter” (the Reynolds number), this has never been experimentally verified. In addition, such an experiment would enable us to determine when or if the statistics would become independent of Reynolds number. For example, in the measurements by Jimenez *et al.* (2010) on the axisymmetric SUBOFF wake, the statistics did not become Reynolds number independent until a Reynolds number based on length of about  $25 \times 10^6$ .

A DARPA SUBOFF 1:240 model is used in order to minimize flow blockage: the blockage will be about 3% for the axisymmetric case. A motorized system to pitch and yaw the model will be used. A traversing system will position the probes anywhere within a cylindrical volume defined by  $0 \leq x/D \leq 32$ ,  $-1.3 \leq r/D \leq 1.3$  and  $-75 \leq \theta \leq 75$ . This system also has the capability of pitching the probes  $\pm 15^\circ$  for calibration purposes, see Figure 22, and it can carry a second probe to allow two-point correlation measurements essential for performing proper orthogonal decomposition. The flow blockage due to the traversing assembly is about 4%. We expect to be able to report the high Reynolds number results taken in this experiment by the time of the conference.

## Acknowledgements

This work was supported by ONR Grant N00014-09-1-0263 (Program Manager Ron Joslin). The 2-D traverse and the cross-wire calibration mechanism were designed and built with the collaboration of Tristen Hohman.



Figure 21. High Reynolds number Test Facility (HRTF).



Figure 22. Three-dimensional traverse mounted in the test section of the HRTF. Jimenez (2007)

## REFERENCES

- Chesnakas C. and Simpson R.L., 1997, Detailed investigation of the three-dimensional separation about a 6:1 prolate spheroid. *AIAA Journal*, 35(6):990–999.
- Delery J.M., 2001, Robert Legendre and Henri Werle: Toward the elucidation of three-dimensional separation, *Annual Review of Fluid Mechanics*, 33:129–154.
- Gross A., Kremheller A. and Fasel H.F., 2011, Simulation of flow over SUBOFF bare hull model, 49th AIAA Aerospace Sciences Meeting, Orlando, Florida.
- Groves, N.C., Huang, T.T. and Chang, M.S., 1989, Geometric characteristics of DARPA SUBOFF Models, DTRC reports, David Taylor Research Centre.
- Jimenez J.M., 2007, High Reynolds Number Flows about Bodies of Revolution with Application to Submarines and Torpedoes, Ph.D. Thesis Princeton University, Princeton, New Jersey.
- Jimenez J.M., Hultmark M. and Smits A.J., 2010, The intermediate wake of a body of revolution at high Reynolds number. *Journal of Fluid Mechanics*, 659:516–539.
- Jimenez J.M., Reynolds R.T. and Smits A.J., 2010, The effects of fins on the intermediate wake of a submarine model. *Journal of Fluids Engineering*, 132:1–7.
- Johansson P.B.V., and George W.K., 2006, The far downstream evolution of the high Reynolds number axisymmetric wake behind a disk. Part I. Single-point statistics. *Journal of Fluid Mechanics*, 555:363–385.
- Karlsson A. and Fureby C., 2009, LES of the flow past a 6:1 prolate spheroid, 47th AIAA Aerospace Sciences Meeting, Orlando, Florida.
- Lloyd, A.R.J.M. and Campbell I.M.C., 1986, Experiments to investigate the vortices shed from a submarine-like body of revolution, 59th meeting of AGARD, Fluid Dynamics Panel Symposium, Monterey, California.
- Bridges, D.H., 2006, The Asymmetric Vortex Wake Problem - Asking the Right Question, 36th AIAA Fluid Dynamics Conference and Exhibit, San Francisco, CA.